Altering lamina assembly reveals lamina-dependent and -independent functions for A-type lamins

Zwerger, Monika ; Roschitzki-Voser, Heidi ; Zbinden, Reto ; Denais, Celine ; Herrmann, Harald ; Lammerding, Jan ; Grütter, Markus G ; Medalia, Ohad

Abstract: Lamins are intermediate filament proteins that form a fibrous meshwork, called the nuclear lamina, between the inner nuclear membrane and peripheral heterochromatin of metazoan cells. The assembly and incorporation of lamin A/C into the lamina, as well as their various functions, are still not well understood. Here, we employed designed ankyrin repeat proteins (DARPins) as new experimental tools for lamin research. We screened for DARPins that specifically bound to lamin A/C, and interfered with lamin assembly in vitro and with incorporation of lamin A/C into the native lamina in living cells. The selected DARPins inhibited lamin assembly and delocalized A-type lamins to the nucleoplasm without modifying lamin expression levels or the amino acid sequence. Using these lamin binders, we demonstrate the importance of proper integration of lamin A/C into the lamina for nuclear mechanical properties and nuclear envelope integrity. Finally, our study provides evidence for cell-type-specific differences in lamin functions.

DOI: https://doi.org/10.1242/jcs.171843

© 2015. Published by The Company of Biologists Ltd | Journal of Cell Science (2015) 128, 3607-3620 doi:10.1242/jcs.171843

RESEARCH ARTICLE

Altering lamina assembly reveals lamina-dependent and -independent functions for A-type lamins

Monika Zwerger[1], Heidi Roschitzki-Voser[1], Reto Zbinden[1], Celine Denais[2], Harald Herrmann[3], Jan Lammerding[2], Markus G. Grütter[1] and Ohad Medalia[1,4,*]

ABSTRACT

Lamins are intermediate filament proteins that form a fibrous meshwork, called the nuclear lamina, between the inner nuclear membrane and peripheral heterochromatin of metazoan cells. The assembly and incorporation of lamin A/C into the lamina, as well as their various functions, are still not well understood. Here, we employed designed ankyrin repeat proteins (DARPins) as new experimental tools for lamin research. We screened for DARPins that specifically bound to lamin A/C, and interfered with lamin assembly *in vitro* and with incorporation of lamin A/C into the native lamina in living cells. The selected DARPins inhibited lamin assembly and delocalized A-type lamins to the nucleoplasm without modifying lamin expression levels or the amino acid sequence. Using these lamin binders, we demonstrate the importance of proper integration of lamin A/C into the lamina for nuclear mechanical properties and nuclear envelope integrity. Finally, our study provides evidence for cell-type-specific differences in lamin functions.

KEY WORDS: DARPins, Assembly, Lamina, Lamins, Nuclear envelope, Nucleus

INTRODUCTION

Lamins assemble into an intricate filamentous meshwork termed the nuclear lamina, a protein layer underlying the inner nuclear membrane (INM) (Dechat et al., 2010b, 2008; Shimi et al., 2008). Four major lamin isoforms constitute the lamina in mammalian cells. Two A-type lamins, lamin A and lamin C (herein referred to as lamin A/C), are alternative splice variants of the *LMNA* gene, whereas the B-type lamins lamin B1 and B2 are encoded by independent genes, *LMNB1* and *LMNB2*, respectively (Lin and Worman, 1993; Peter et al., 1989; Vorburger et al., 1989). A-type lamins are mainly expressed in differentiated cells, whereas all nucleated cells express at least one B-type lamin throughout all developmental stages (Worman et al., 1988).

One major function of lamins is to mechanically support the nuclear envelope and to determine the mechanoelastic properties of nuclei. However, lamin A/C was found to also participate, directly or indirectly, in major nuclear processes, including chromatin organization, transcriptional regulation, cell proliferation, DNA replication and repair, as well as stem cell maintenance and differentiation (reviewed in Dechat et al., 2010a). Despite extensive research, the various functions of these proteins have remained imprecisely defined (Burke and Stewart, 2013). Cell-type-specific lamina composition, as well as differential expression of interaction partners at the nuclear envelope, might account for the different roles of lamins in specific tissues, and thus might explain conflicting results and imprecise definitions of lamin functions.

Regardless of the progress in the development and improvement of microscopy techniques, the assembly of lamins and the structural organization of the lamina in somatic cells is still largely elusive (Zwerger and Medalia, 2013). All lamins display a conserved tripartite structure, comprising a central α-helical rod domain flanked by a short head domain and a tail domain with a nuclear localization signal, as well as an immunoglobulin (Ig)-fold (Dhe-Paganon et al., 2002; Loewinger and McKeon, 1988; Shumaker et al., 2005). Based on *in vitro* studies, it has been suggested that lamins, like all intermediate filament (IF) proteins, form approximately 50-nm long dimers arising from two parallel monomers that interact through a central coiled-coil-forming domain (Herrmann et al., 2007; Parry, 2005). Lamin dimers interact longitudinally through head-to-tail association to form a long polar polymer of dimers that can further assemble laterally into high-molecular-mass structures (Aebi et al., 1986; Ben-Harush et al., 2009; Goldberg et al., 2008; Herrmann and Aebi, 2004; Stick and Goldberg, 2010). On the cellular level, light microscopy data and biochemical fractionation experiments indicate that different lamin isoforms assemble into separate but interconnected networks (Kolb et al., 2011; Shimi et al., 2008). Notably, a small fraction of lamins (approximately 10% of A-type lamins) also localizes within the nuclear interior, where they interact with numerous nuclear binding partners (Dorner et al., 2007; Kolb et al., 2011). Although these nucleoplasmic lamins display higher mobility, their oligomeric state is yet undefined (Shimi et al., 2008). The term 'lamina' thus defines assembled lamins at the nuclear envelope, whereas the term 'nucleoplasmic lamins' refers to lamins within the nuclear interior. It has so far remained unclear whether these two lamin populations exert different functions in the nucleus.

In order to gain a deeper understanding of the mechanisms underlying lamin functions and assembly, as well as the effects of mutations, novel tools need to be devised and employed to circumvent current limitations. In contrast to IF proteins, for which no specific polymerization inhibitors have been characterized as of yet, a multitude of such inhibitors exist for microtubules and actin filaments, and their discovery has led to major breakthroughs in these fields of research (Pollard, 2007; Svitkina and Borisy, 1999). Such tools have enabled the study of actin dynamics, and the first crystal structures were determined for globular actin in complexes with deoxyribonuclease I, gelsolin or profilin, which all prevent its polymerization (Otterbein et al., 2001). In analogy to the actin field, inhibition of lamin polymerization in cells would allow for deeper

[1]Department of Biochemistry, University of Zurich, Winterthurerstrasse 190, Zurich 8057, Switzerland. [2]Cornell University, Weill Institute for Cell and Molecular Biology, Department of Biomedical Engineering, Weill Hall, Ithaca, NY 14853, USA. [3]Functional Architecture of the Cell, German Cancer Research Center (DKFZ), Heidelberg 69120, Germany. [4]Department of Life Sciences and the National Institute for Biotechnology in the Negev, Ben-Gurion University, Beer-Sheva 84105, Israel.

*Author for correspondence (omedalia@bioc.uzh.ch)

Received 19 March 2015; Accepted 13 August 2015

Journal of Cell Science (2015) 128, 3607-3620 doi:10.1242/jcs.171843

insights into lamina assembly *in vivo*, and enable us to decipher the roles of lamina incorporation for various lamin functions, without introducing mutations or interfering with the expression levels of lamins.

In this study, we decided to screen for lamin-specific binding proteins using a library of designed ankyrin repeat proteins (DARPins) (Binz et al., 2004). DARPins are small (approximately 18 kDa) engineered proteins that can be selected to bind precisely and with high affinity to certain subdomains of lamin proteins, and can thus interfere with binding of lamins to specific interaction partners or with lamin self-assembly. Here, we describe the selection and characterization of high-affinity DARPins that target lamin A/C and specifically inhibit lamin oligomerization. These DARPins can be utilized as tools to either interfere with lamin A oligomerization *in vitro*, or to inhibit the incorporation of lamin A/C into the lamina *in vivo*. By expressing DARPins in cultured cells, we demonstrate the importance of incorporation of lamin A/C into the lamina for nuclear envelope integrity, nuclear stiffness and morphology.

In summary, the DARPins employed in our study provide a powerful tool to study aspects of lamin A/C and the nuclear lamina that have been, so far, difficult to address.

RESULTS

There are currently only few molecular tools available to selectively interfere with the assembly or functions of IF proteins. Therefore, we made use of DARPin technology to generate specific and robust binders of lamin A that can be used as tools for studying these proteins, in particular their assembly and functions, *in vitro* as well as *in vivo*.

Identification of selective DARPin binders of human lamin A that interfere with lamin A assembly

The selection of DARPins that specifically bind to lamin A was performed with standard ribosome display using an N_3C library (Seeger et al., 2013). As the target protein, we used recombinant human lamin A that had been reconstituted in dimerization buffer (Taimen et al., 2009). After four ribosome-display selection rounds, DARPins were analyzed for target binding by crude cell extract enzyme-linked immunosorbent assay (ELISA). We expressed and purified the 19 most promising candidates and used surface plasmon resonance to determine the properties of their binding to lamin A. Sixteen candidates showed binding constants that were mostly in the low nanomolar range (supplementary material Table S1) and were therefore considered as high-affinity binders for human lamin A.

We next screened for DARPins that not only bound to the protein but also interfered with lamin A polymerization. First, we analyzed the effect of DARPins on lamin assembly *in vitro*. Human lamin A that had been purified and reconstituted in dimerization buffer was incubated with lamin-A-specific DARPins, or a control DARPin that had been randomly chosen from the library [E3_5 (Binz et al., 2006)] and does not bind to lamin A (supplementary material Fig. S2A,B, Fig. S4A,B). Lamin assembly was then initiated through stepwise dialysis into buffers with reduced ionic strength and analyzed by centrifugation. High-molecular-mass assemblies sediment into the pellet, whereas lamins in low-oligomeric states remain in the supernatant (Aebi et al., 1986). From the set of selected DARPins, four of them inhibited lamin assembly, retaining lamin A in the supernatant after centrifugation (DARPins LaA_3, LaA_4, LaA_5 and LaA_9), two had a mild impact on assembly (LaA_6 and LaA_19) and 13 DARPins did not affect assembly

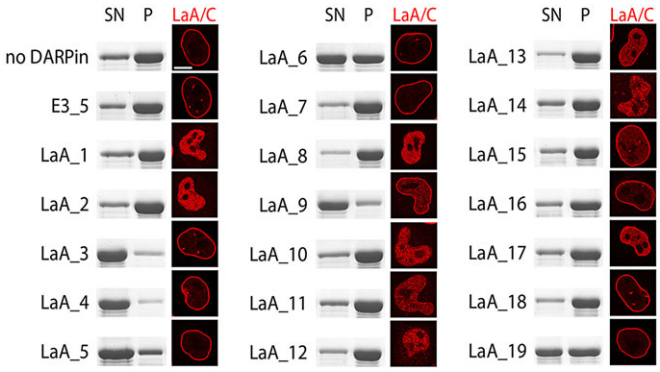

Fig. 1. DARPins selected to bind to lamin A can alter lamin assembly *in vitro* and *in vivo*. Left panels, lamin A *in vitro* assembly was performed in the absence of DARPins (no DARPin, buffer), in the presence of a control DARPin (E3_5) or in the presence of the indicated DARPins that specifically bound to human lamin A. Samples were centrifuged for 35 min at 50,000 ***g***, and the supernatant (SN) and pellet (P) fractions were analyzed by SDS PAGE and staining with Coomassie Blue. Right panels, confocal images of HeLa-K cells that stably expressed DARPins and were immunostained for lamin A/C (red). DARPin-expressing cells were identified by the bicistronic expression of EGFP (not shown). Scale bar: 10 µm.

(Fig. 1; supplementary material Fig. S1A). The strongest inhibition of lamin A assembly *in vitro* was detected with DARPins LaA_3 and LaA_4.

Lamin A/C contain dozens of modification sites – e.g. phosphorylation and acetylation sites – that can change their biochemical properties *in vivo*. Therefore, we studied the effect of DARPins on lamin A/C assembly in mammalian cells. We stably expressed DARPins specific for lamin A in HeLa-K cells and monitored the localization of lamin A/C through immunofluorescence (Fig. 1). Although some DARPins had no effect on the localization of lamin A/C at the nuclear envelope, several DARPins caused a substantial delocalization of lamin A/C to the nuclear interior. The highest levels of delocalization, based on immunofluorescence microscopy and fluorescence intensity measurements, were found in cells that expressed DARPins LaA_1 and LaA_2 (supplementary material Fig. S1B,C). Interestingly, these DARPins did not affect lamin assembly *in vitro*, whereas the DARPins that prevented the assembly of high-molecular-mass complexes *in vitro* – e.g. LaA_3 and LaA_4 – did not show substantial effects on lamin A/C localization *in vivo* (Fig. 1).

To assess whether the influence of DARPins LaA_1 and LaA_2 on lamin A/C localization was a direct effect caused by the DARPin interactions with A-type lamins, we tested whether these DARPins bound to additional cellular proteins – other than lamin A/C – *in vivo*. Therefore, we performed a co-immunoprecipitation assay using HeLa-K cells that stably expressed mCherry-tagged DARPins, and analyzed the DARPin-interacting proteins by western blot analysis and mass spectrometry (supplementary material Fig. S2). As expected, all four lamin-A/C-specific DARPins interacted with two major proteins (supplementary material Fig. S2A) – lamin A and lamin C (supplementary material Fig. S2B,C).

DARPin inhibitors do not alter A-type lamin protein levels, but do affect lamin subnuclear localization and assembly state

To determine the cellular effects of A-type lamin redistribution from the lamina to the nucleoplasm, we generated a panel of modified U2OS cells (Fig. 2A). These cells expressed the lamin-A-specific DARPins LaA_1 and LaA_2 (which caused a redistribution of A-type lamins from the nuclear envelope in

Journal of Cell Science (2015) 128, 3607-3620 doi:10.1242/jcs.171843

HeLa-K cells), or LaA_3 and LaA_4 (which did not affect the localization of A-type lamins in HeLa-K cells). Notably, cells with nucleoplasm enriched for A-type lamins were viable and proliferated normally (data not shown).

As observed for HeLa-K cells, expression of DARPins LaA_1 and LaA_2 in U2OS cells resulted in a redistribution of lamin A/C to the nucleoplasm, which was associated with a high fraction of irregularly shaped nuclei. By contrast, lamin A/C localized normally to the nuclear rim in cells that expressed the DARPins LaA_3 and LaA_4 (Fig. 1, Fig. 2A). These observations confirm that DARPins LaA_1 and LaA_2, but not LaA_3 and LaA_4, alter lamina assembly *in vivo*.

Importantly, neither the localization of B-type lamins, of the lamin-binding proteins Lap2α, Lap2β, LBR, nor of diverse markers for euchromatin and heterochromatin were altered as a result of delocalization of lamin A/C to the nucleoplasm through DARPins LaA_1 and LaA_2 (Fig. 2A, data not shown). However, we observed a redistribution of emerin from the nuclear envelope to the cytoplasm in cells that expressed DARPins LaA_1 and LaA_2. The same phenotype was observed in U2OS cells that had depleted levels of A-type lamins as a result of RNA interference (RNAi) (Fig. 2A). Moreover, the mislocalization of emerin was confirmed in HeLa-K cells that stably expressed DARPins LaA_1 and LaA_2 (data not shown). Our observations thus indicate that anchorage of emerin to the INM depends not only on the presence of lamin A/C (Nagano et al., 1996; Sullivan et al., 1999) but also on its incorporation into the nuclear lamina.

Next, we analyzed the polymerization state of the A-type lamins in cells that expressed DARPins LaA_1 and LaA_2. Cells from the panel of modified U2OS were incubated in mild extraction buffer containing 0.2% NP40, and then centrifuged, and supernatants containing the extracted proteins, as well as the pellets, were analyzed by western blotting (Fig. 2B). This differential extraction experiment confirmed that a large fraction of A-type lamins – i.e. more than 40% of the total lamin A or lamin C fraction – was found in the supernatant of cells that expressed the DARPins LaA_1 or LaA_2, even after centrifugation at 50,000 ***g*** (Fig. 2B,C; supplementary material Fig. S3A). By contrast, more than 90% of the lamin A and lamin C fraction was found in the pellets from all other cell lines, including U2OS cells that expressed LaA_3 and LaA_4. B-type lamins could not be extracted under these conditions from any cell line (Fig. 2B). These results indicate that the nucleoplasmic lamins, as a result of DARPins LaA_1 and LaA_2, are not assembled into large filaments and are not tightly associated with nuclear proteins or high-molecular-mass complexes.

Despite their altered assembly state and localization, the protein levels of A-type lamins remained almost unchanged in cells that expressed DARPins LaA_1, LaA_2, LaA_3 and LaA_4 (Fig. 2D; supplementary material Fig. S3B,C). The protein levels of B-type lamins and the lamin-binding proteins emerin, Lap2α and LBR were also comparable in all cell lines. In summary, the presence of DARPins LaA_1 and LaA_2 interferes with the incorporation of A-type lamins into the lamina and causes a redistribution of emerin to the endoplasmic reticulum (ER). Moreover, a large fraction of the A-type-lamin–DARPin complexes in the nucleoplasm exist in a non-polymerized state.

DARPin–lamin complexes remain in the nucleoplasm at the end of mitosis and retain a high level of phosphorylation at Ser22

We next assessed whether DARPins LaA_1 and LaA_2 have the potential to cause delocalization of A-type lamins from an assembled lamina network. Alternatively, they might bind to nucleoplasmic A-type lamins during mitosis and prevent their integration into the lamina during nuclear envelope reassembly. As a first step, we investigated the effect of DARPin LaA_1 on interphase HeLa-K cells that stably expressed green fluorescent protein (GFP)tagged lamin-A (GFP–lamin-A). These cells were briefly permeabilized with detergent to allow penetration, then incubated with mCherry-tagged LaA_1. The DARPin mCherry–LaA_1 bound to the lamins at the nuclear envelope but did not cause a delocalization of GFP–lamin-A to the nucleoplasm over a period of 60 min, indicating that DARPin binding did not affect crucial GFP–lamin-A interactions at the nuclear envelope (Fig. 3A). Next, we transiently expressed mCherry–LaA_1 in these HeLa-K cells and monitored the reassembly of GFP–lamin-A at the end of mitosis. In cells that displayed an increase in mCherry–LaA_1 levels during mitosis, GFP–lamin-A failed to re-integrate into the lamina (Fig. 3B, arrowheads), whereas GFP–lamin-A reassembled normally into the lamina of untransfected daughter cells (Fig. 3B, asterisks). Thus, we conclude that DARPin LaA_1 binds to A-type lamins in the lamina but does not mediate their delocalization into the nucleoplasm; rather, LaA_1 prevents unassembled A-type lamins from re-associating with the lamina at the end of mitosis.

Lamina reassembly is usually initiated by the activity of mitotic phosphatases that remove the mitotic phosphate groups from A-type lamins in late anaphase to early telophase (Thompson et al., 1997; Wurzenberger and Gerlich, 2011). The Ser22 residue in lamin A/C is one of four major amino acids that are hyperphosphorylated during mitosis, but it is also a high-turnover site during interphase. Moreover, the phosphorylation state of Ser22 influences subnuclear localization of lamin A/C (Buxboim et al., 2014; Heald and McKeon, 1990; Kochin et al., 2014). Interestingly, U2OS cells that expressed LaA_1 and LaA_2 displayed a higher level of phosphorylation at Ser22 compared to control cells, indicating that the subnuclear localization of A-type lamins correlates with Ser22 phosphorylation status (Fig. 3C). We, however, cannot exclude the possibility that high levels of phosphorylation at Ser22 are linked to a certain degree of degradation in the case of cells expressing the DARPins LaA_1 and LaA_2 (Fig. 3C,D) (Buxboim et al., 2014). In summary, DARPin LaA_1 binds to both assembled A-type lamins at the nuclear envelope as well as nucleoplasmic lamin A/C during mitosis, and the latter prevents their incorporation into the lamina after mitosis. These nucleoplasmic A-type lamins display increased Ser22 phosphorylation.

Lamin A/C associated with the lamina is required for nuclear envelope and chromatin organization in human dermal fibroblasts

The experimental system we generated through modification of U2OS cells allows us to differentiate between lamina-dependent and lamina-independent lamin A/C functions. It has been previously reported, however, that cancer cells such as HeLa-K or U2OS are less sensitive to alterations of lamin levels than non-cancer cells (Dorner et al., 2006; Pekovic et al., 2007). We, therefore, extended our studies to investigate the effects of DARPins on immortalized human dermal fibroblasts (HDFs). As control cells, we used a fibroblast cell line isolated from an individual homozygous for the *LMNA* Y259X mutation that completely lacks A-type lamins. It was previously shown that a subset of these HDF Y259X cells display abnormally shaped nuclei with altered chromatin organization and gross nuclear envelope alterations, including nuclear envelope areas in which B-type lamins, emerin, nesprin-1, LAP2β and Nup153 were undetectable (Muchir et al., 2004; van Engelen et al., 2005).

Journal of Cell Science (2015) 128, 3607-3620 doi:10.1242/jcs.171843

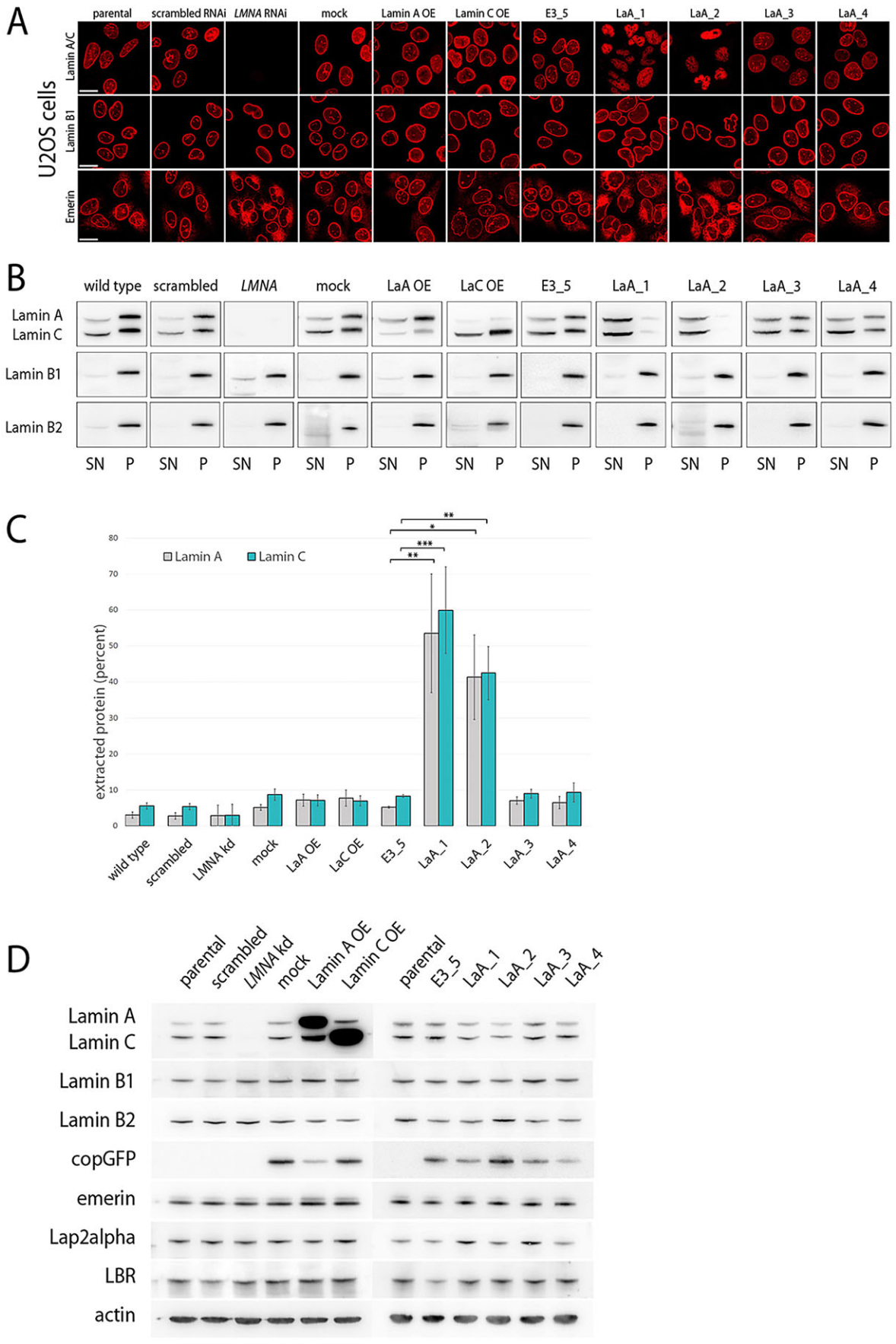

Fig. 2. See next page for legend.

Journal of Cell Science (2015) 128, 3607-3620 doi:10.1242/jcs.171843

Fig. 2. *In vivo* inhibitors do not alter A-type lamin protein levels but do alter their subnuclear localization and assembly state. (A) Confocal images of wild-type U2OS cells and cells that stably expressed a scrambled small interfering (si)RNA (scrambled RNAi), an siRNA for *LMNA* silencing (*LMNA* RNAi, *LMNA* in B, LMNA kd in C), the empty lentiviral plasmid (mock), lamin A (lamin A OE), lamin C (lamin C OE), the control DARPin E3_5, or the indicated different lamin A-specific DARPins (LaA_x, where x is the DARPin identifier). Cells were immunostained with antibodies against lamin A/C, lamin B1 and emerin. Scale bars: 20 µm. (B) Western blot analysis of the supernatant (SN) and pellet fractions (P) of wild-type and modified U2OS cells shown in A after extraction with a buffer containing 0.2% NP40 and using antibodies against lamin A/C, lamin B1 and lamin B2. Note that the supernatant and pellet were loaded in a 10:1 ratio. (C) Statistical analysis of the ratio of extracted to total lamin A and lamin C in different U2OS cell lines. The average of three individual experiments±s.e.m. is shown. Statistical significance was calculated using a one-way ANOVA test followed by Bonferroni's multiple comparison test, where $*P \leq 0.05$, $**P \leq 0.01$ and $***P \leq 0.001$. (D) Western blot analysis of lamin and lamin-binding protein levels in the wild-type and modified U2OS cells shown in A. The levels of exogenous lamin A, lamin C, and of DARPin expression is reflected by levels of bicistronically expressed copGFP, a green fluorescent protein cloned from *Pontellina plumata*. β-actin was used as loading control.

Surprisingly, similar effects were observed in a subset of HDF cells that expressed the DARPins LaA_1 and LaA_2 (Fig. 4A). As expected, in HDFs that expressed these DARPins, A-type lamins were distributed throughout the nucleoplasm. In these cells, we often observed nuclei in which the nuclear envelope composition at one or both poles appeared to be grossly altered (Fig. 4A, arrows). In particular, lamin B1, Lap2β and nuclear pore complexes (NPCs) were absent in these areas but localized normally in neighboring nuclear envelope areas of the same nucleus. DNA labeling using Hoechst 33342 stain displayed either weak chromatin staining or granular staining, indicating altered chromatin structure at dysmorphic nuclear poles. Emerin was found to be largely mislocalized from the nuclear envelope to the cytoplasm. Disturbed nuclear envelope composition at nuclear poles was rarely detected in HDFs that expressed the DARPins LaA_3 and LaA_4 (Fig. 4B). As reported for HDF Y259X cells, the fraction of cells displaying these nuclear envelope disruptions decreased with increasing passage number, indicating that these cells either divided more slowly in comparison to cells with intact nuclei, or that the integrity of the nuclear envelope was restored in some of these cells. In our experiments, the decrease in the number of cells with a disrupted nuclear envelope was accompanied by a decline in the number of nuclei in which A-type lamins localized to the nucleoplasm, despite selection pressure on DARPin expression (Fig. 4B). However, among the cells with nucleoplasmic A-type lamin localization, the fraction of disrupted nuclear envelopes remained high (>50%, Fig. 4C).

These combined observations led us to conclude that cells in which nuclear envelope localization of A-type lamins was restored (e.g. cells with low DARPin expression) have a growth advantage over those with mainly nucleoplasmic A-type lamins. Furthermore, cells with nucleoplasmic A-type lamins were prone to nuclear envelope damage, independent of the passage number (Fig. 4C). In summary, HDF but not cancer cells displayed major nuclear envelope alterations that were comparable to the knockout phenotype, indicating that lamina-associated A-type lamins are required for nuclear integrity in this cell type.

The contributions of A-type lamins to nuclear mechanical properties are mostly lamina-dependent

Studies on wild-type and lamin-deficient mouse embryonic fibroblasts (MEFs) have previously shown that lamin A is a major determinant of nuclear stiffness and that loss of A-type lamins leads to more deformable and more fragile nuclei (Buxboim et al., 2014; Lammerding et al., 2006, 2004; Swift et al., 2013). It has so far remained unclear, however, whether nuclear stiffness is determined solely by lamina-associated lamins or whether nucleoplasmic lamins also contribute, possibly by forming a nucleoplasmic scaffold or by influencing chromatin organization.

As we had observed a high fraction of misshapen nuclei in HeLa-K and U2OS cells in which A-type lamins was delocalized to the nucleoplasm (Fig. 1, Fig. 2A), we next studied the effects of lamin A/C nuclear localization on the mechanical properties of nuclei. We quantified the alterations in the shape of the nuclei by computing the nuclear contour ratio ($4\pi \times \text{area/perimeter}^2$), an established measurement of nuclear shape (Lammerding et al., 2005). The contour ratio approaches the value of 1 with increasing roundness of a nucleus, whereas the value decreases with increasing convoluted nuclear morphology. HeLa-K cells and those expressing the control DARPin E3_5 had very similar nuclear contour ratios (0.79 for both cell lines). Cells that expressed LaA_1 and LaA_2, despite normal levels of lamin A expression, displayed abnormal nuclear shapes with nuclear contour ratio values comparable to those of knockout cells (0.70, 0.68 and 0.68 for LaA_1, LaA_2 and *LMNA* knockdown, respectively; Fig. 5A; supplementary material Fig. S3B). This observation demonstrates that lamina-incorporation of lamin A/C is required to maintain nuclear morphology. The shapes of nuclei in cells that expressed DARPins LaA_3 and LaA_4 were comparable to those in control cells.

Abnormal nuclear morphology is often caused by decreased nuclear stiffness, as has been demonstrated previously in HDFs and MEFs that express laminopathic mutations or that lack lamin A/C (Zwerger et al., 2013). We therefore studied nuclear stiffness by analyzing the nuclear deformability of wild-type HeLa-K and HeLa-K cells that expressed the different DARPins. For this study, cells were grown on transparent silicone membranes and imaged before and during the application of strain to the elastic silicone membrane (Fig. 5B). Nuclei of HeLa-K that expressed DARPins LaA_1 and LaA_2, in which A-type lamins are mostly absent from the nuclear envelope, deformed about 25% compared to the deformation of the entire cell, whereas nuclei of control cells deformed, on average, by 10% compared to the deformation of the entire cell (Fig. 5B,C). Thus, changes in A-type lamin localization and assembly alone are sufficient to modulate nuclear stiffness, and the nuclear lamina network apparently plays a major role in providing structural support. However, HeLa-K cells with knockdown of *LMNA* displayed even more deformable nuclei than cells expressing DARPins LaA_1 and LaA_2, with an average value of more than 40% relative to the deformation of the entire cell. These results suggest that the lamina-incorporated lamins contribute to nuclear stiffness but that nucleoplasmic lamins play a role in nuclear stiffening as well, presumably mediated by scaffolding effects through interactions with multiple nuclear components or by more indirect mechanisms, such as modulating global chromatin structure.

DARPins selected for lamin A bind one of two major epitopes

To characterize the interactions of DARPins with human lamin A on a molecular basis and to understand the different cellular effects described above, we mapped the specific epitopes of DARPins LaA_1 to LaA_4 on lamin A. Mature lamin A or various lamin A fragments were immobilized on membranes and probed with these DARPin candidates, which was followed by western blotting to detect DARPins bound to the lamin variants (supplementary

Journal of Cell Science (2015) 128, 3607-3620 doi:10.1242/jcs.171843

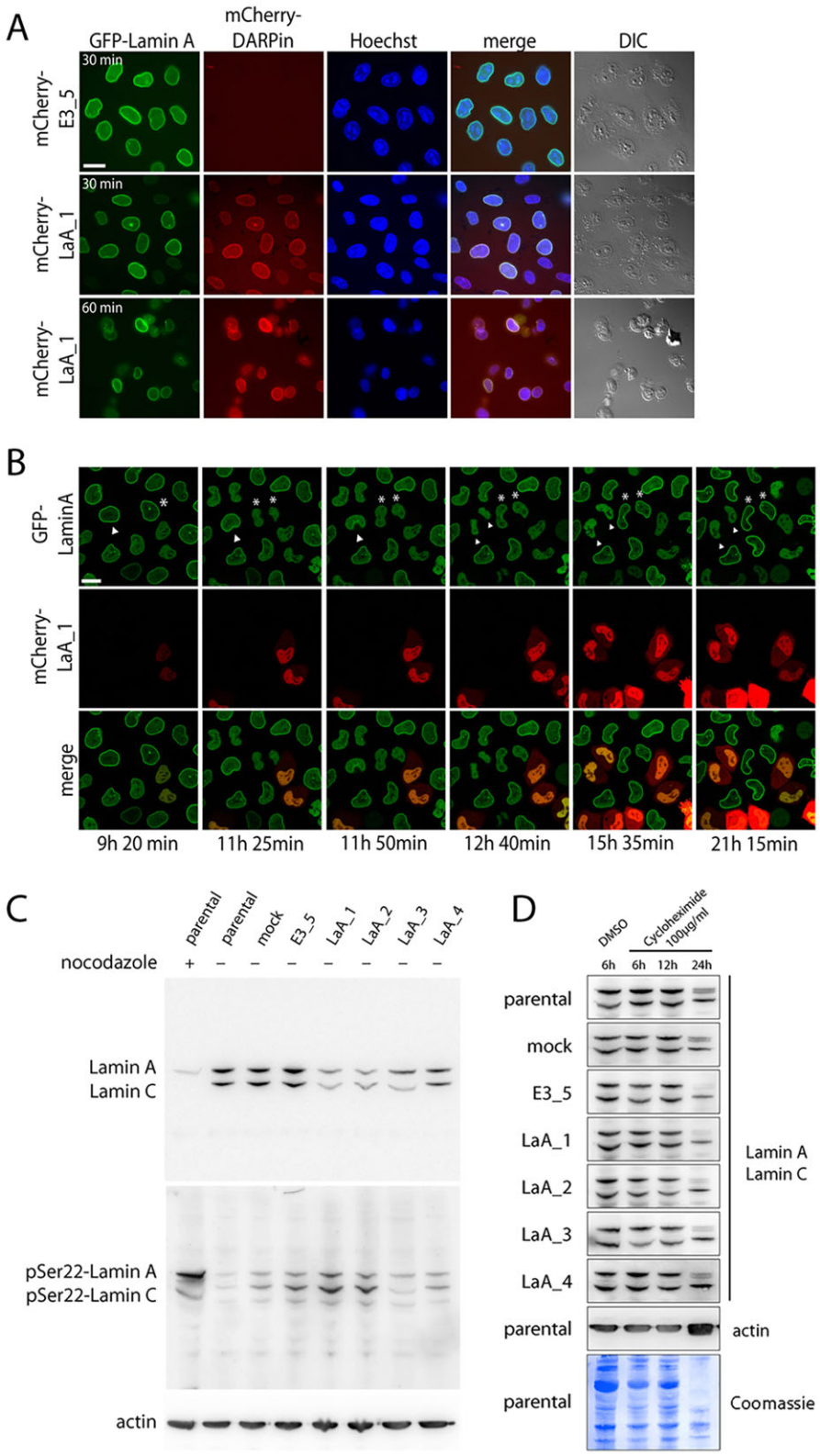

Fig. 3. A-type lamins delocalize to the nucleoplasm post-mitotically and retain a high level of phosphorylation. (A) HeLa-K cells that stably expressed GFP–lamin-A were incubated with mCherry-tagged DARPins E3_5 or LaA_1, and Hoechst 33342 stain for up to 60 min, after brief incubation with Triton X–100 to allow penetration of the DARPins into the cells. Scale bar: 20 µm. (B) Live-cell imaging of HeLa-K cells that stably expressed GFP–laminA and had been transfected with mCherry–DARPin LaA_1. GFP–lamin-A reassociated with the lamina in non-transfected daughter cells (marked with asterisks), whereas expression of mCherry- LaA_1 blocked GFP–lamin-A reassembly after mitosis (marked with arrowheads). Scale bar: 20 µm. (C) Western blot analysis of wild-type and modified U2OS cells to detect A-type lamins, as well as A-type lamins phosphorylated at amino acid Ser22. Nocodazole-treated cells were used as a control for phosphorylation, β-actin was used as loading control. (D) Western blot analysis of wild-type and modified U2OS cells treated with cycloheximide for the indicated time points or DMSO to detect degradation of A-type lamins. β-actin was used as control for a stable protein, and the Coomassie-stained membrane shows the efficiency of cycloheximide treatment. In D, the upper band represents lamin A and the lower band represents lamin C.

material Fig. S4A). These experiments revealed two main binding epitopes that are recognized by the selected DARPins (supplementary material Fig. S4A; summarized in Fig. 6). DARPins LaA_1 and LaA_2 bound to amino acid residues 113–140 of lamin A, a region within the coil-1B domain, whereas DARPins LaA_3 and LaA_4 bound to a segment that includes the head and coil 1A of the rod domain (amino acid residues 1–62). Notably, the interactions of the DARPins LaA_3 and LaA_4 with lamin A depend on the lysine residue at position 32 of lamin A (supplementary material Fig. S4A; Fig. 6). Lamin A and lamin C are alternative splice variants from the same gene that differ at their C-termini, but are identical over the first 566 amino acids. DARPins

Journal of Cell Science (2015) 128, 3607-3620 doi:10.1242/jcs.171843

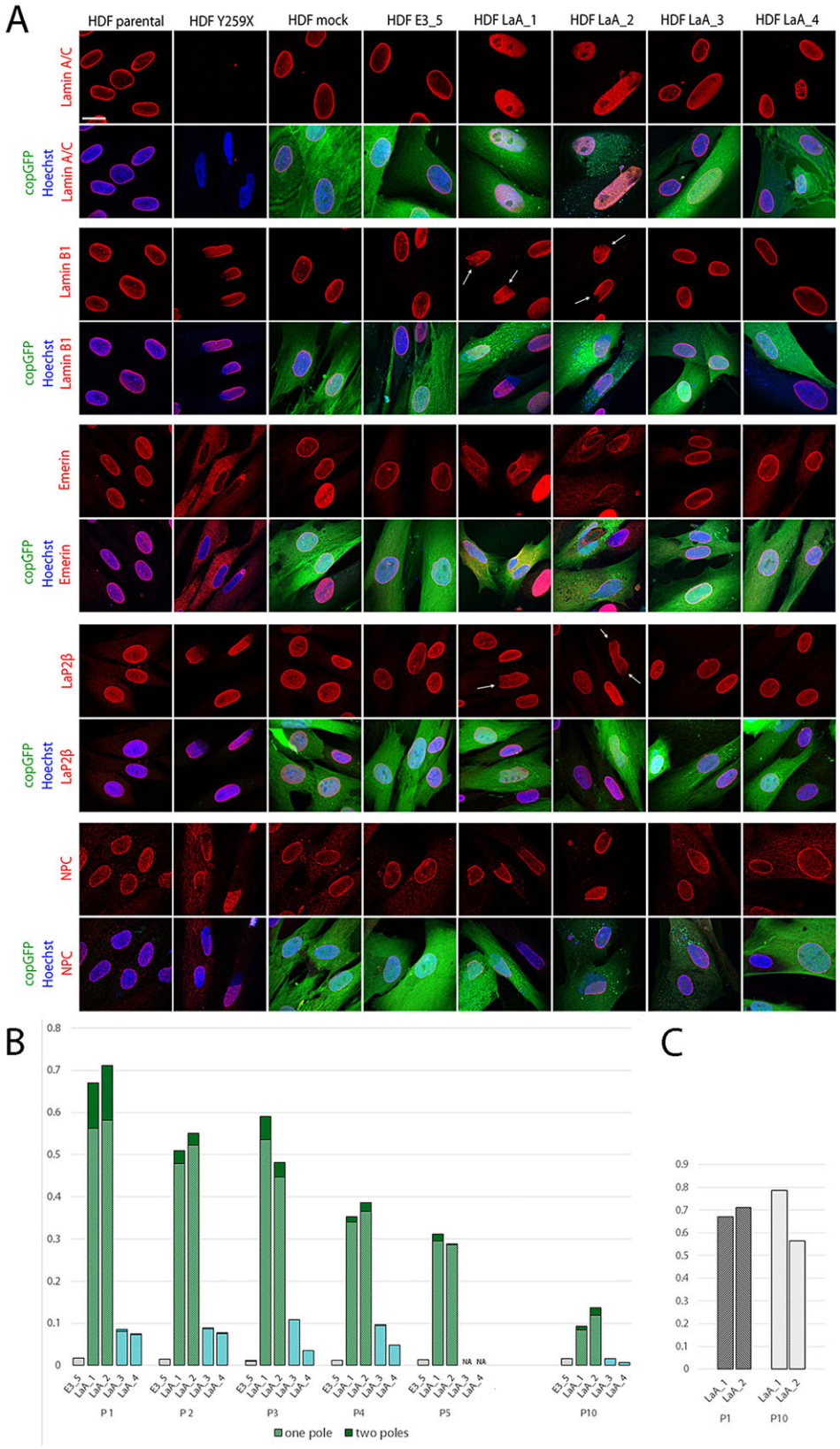

Fig. 4. HDFs with A-type lamin delocalization display gross nuclear envelope and chromatin alterations. (A) Confocal images of wild-type HDFs, HDFs homozygous for the mutation Y259X, which completely lack A-type lamins, and HDFs that stably expressed the empty lentiviral plasmid (mock), the control DARPin E3_5, or the indicated different lamin-A-specific DARPins. Cells were immunostained with antibodies against lamin A/C, lamin B1, emerin, Lap2β or nuclear pore complexes (NPCs). Lentiviral vectors contain an internal ribosome entry site (IRES) site followed by the coding sequence for copGFP for bicistronic expression. Consequently, the green copGFP signal directly correlates with DARPin expression levels. Arrows indicate nuclear poles in which the nuclear envelope composition appears to be grossly altered. Scale bar: 20 µm. (B) Statistical analysis of the percentage of nuclei displaying disrupted nuclear envelope organization at one (light grey for E3_5 control, green or turquoise for DARPins that do or do not cause A-type lamin delocalization, respectively, bottom of columns) or both poles (dark grey, and green or turquoise, top of columns), as determined by staining for lamin B1, and at different passages (P) after viral transduction. At least 300 cells were analyzed per data point. (C) Statistical analysis of the percentage of nuclei displaying disrupted nuclear envelope organization (as determined after staining for lamin B1) among cells in which A-type lamins delocalized to the nuclear interior (as determined by staining for lamin A/C) at passages 1 and 10. NA, not applicable.

LaA_1, LaA_2, LaA_3 and LaA_4 therefore bind, as expected, to both A-type lamin isoforms. We observed very weak binding of DARPins LaA_1 and LaA_2, and moderate binding of DARPins LaA_3 and LaA_4 to lamin B1 and lamin B2, and only weak affinity, at most, to other members of the IF protein family (supplementary material Fig. S4B,C). In summary, the DARPins selected for our study bind with high affinity and specificity to human lamin A/C at two distinct regions – the extended head domain and coil 1B. Furthermore, the binding to these regions specifically alters the localization and assembly properties of A-type

Journal of Cell Science

Journal of Cell Science (2015) 128, 3607-3620 doi:10.1242/jcs.171843

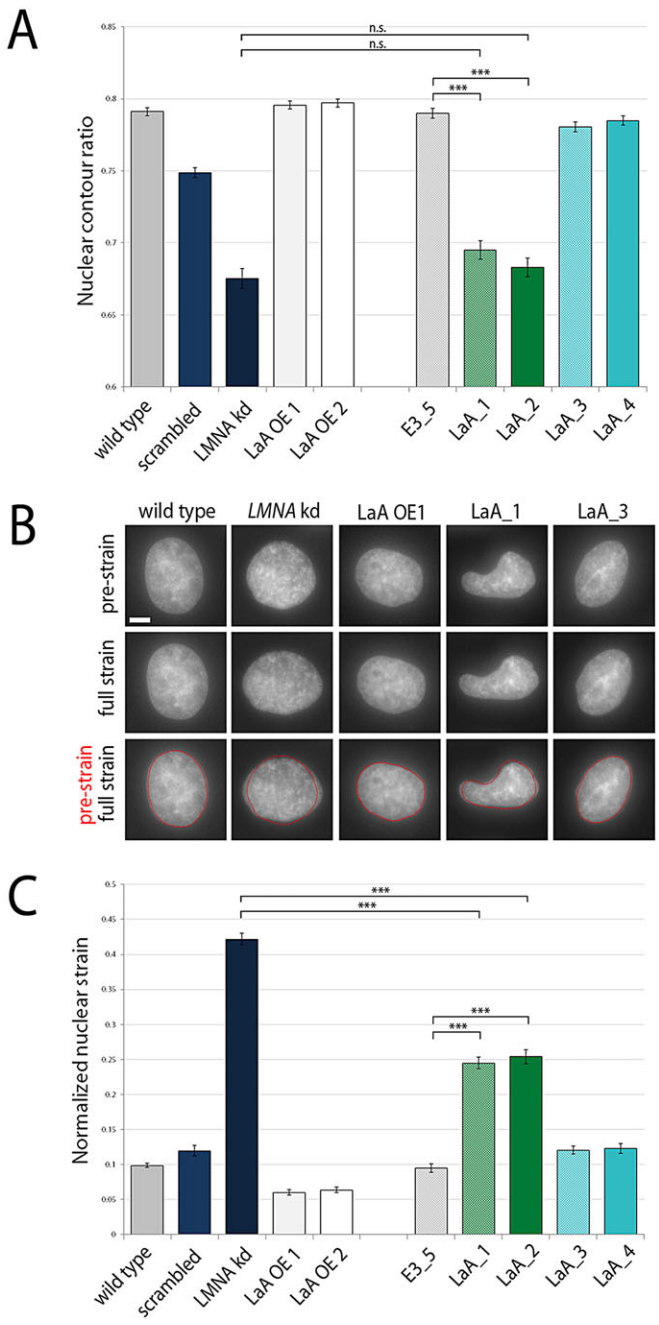

Fig. 5. Nuclear mechanical properties are impaired if A-type lamins are not incorporated into the lamina. (A) Quantitative analysis of nuclear roundness by assessing the nuclear contour ratio of wild-type HeLa-K cells and cells that stably expressed GFP–lamin-A at low and high expression levels (LaA OE 1 and LaA OE 2, respectively), a scrambled siRNA, an siRNA to induce *LMNA* silencing (LMNA kd), the control DARPin E3_5, or the indicated different lamin-A-specific DARPins. Values represent the average nuclear contour ratio of >300 nuclei±s.e.m. (B) Changes in the nuclear shape of unstretched (pre-strain, upper panel) and fully stretched (full strain, middle panel) wild-type and the modified HeLa-K cells. Images in the lower panels represent nuclei under strain, overlaid with the nuclear contour from the pre-stretch state in red. Scale bar: 5 µm. (C) Statistical analysis of nuclear deformation of wild-type and modified HeLa-K cells. Values represent the average normalized nuclear strain (inferred from the ratio of induced nuclear strain to the applied membrane strain) of ≥100 nuclei±s.e.m. Statistical significance in A and C was calculated using a one-way ANOVA test followed by Bonferroni's multiple comparison test. A *P*-value of >0.05 was considered as not significant (n.s.); ***$P \leq 0.001$.

lamins. The combined results of this study and the effects of different DARPins are summarized in Fig. 7.

DISCUSSION

Despite the wealth of information on lamins and components of the nuclear lamina, their diverse functions remain only incompletely understood. Detailed insights into lamin assembly and functions are fundamental for understanding the regulation of nuclear processes and mechanical properties, but also essential for deciphering the causes and effects of many diseases. During the past 25 years, more than 400 mutations within the *LMNA* gene have been identified that cause at least 12 distinct diseases, collectively termed laminopathies (Worman, 2012). Laminopathies include muscular dystrophies, as well as the premature aging disease Hutchison Gilford progeria syndrome (Bertrand et al., 2011; Pereira et al., 2008; Worman, 2012). Currently, the lack of tools for altering the binding and biochemical properties of lamins, and consequently the lamina, present a limiting step in deciphering the precise functional and structural aspects of these important cellular elements.

We describe here a set of DARPins that bind with high affinity and specificity to either the N-terminal domain or to the central rod domain of lamin A and lamin C. Expression of DARPins in living cells prevents lamin A/C from polymerization and lamina incorporation, which enables studying the role of lamina assembly for lamin A/C functions (Fig. 7). DARPins thus represent an elegant approach to alter assembly of these nuclear IF proteins *in vitro* as well as *in vivo*, and to address important open questions in the lamin field.

Binding of DARPins to the head domain of lamin A inhibits assembly *in vitro*

In vitro analysis of lamins suggests that lamin dimers interact longitudinally to form head-to-tail polymers of dimers. This initial process is dependent on the head domain of lamin A (Isobe et al., 2007; Spann et al., 1997), thus proteins that bind with high affinity to the N-terminus of lamin A/C are expected to inhibit their assembly. Here, we have identified DARPins that specifically bind to the head domain and coil 1A (amino acids 1–62) of human lamin A, with Lys32 as an amino acid that is crucial for their binding (Fig. 6; supplementary material Fig. S4A). Notably, it is very possible that the actual binding epitope for DARPins LaA_3 and LaA_4 comprises a shorter stretch than amino acids 1–62 – e.g. only the head domain – but that these DARPins bind only to dimerized lamin A. Consequently, additional amino acids from the central rod might be required, not necessarily for the interaction itself but for dimerization of the fragments.

DARPins LaA_3 and LaA_4 inhibit the formation of large lamin A assemblies, as lamin A was recovered from the supernatant after centrifugation (Fig. 1). The fact that DARPins that bind to the N-terminus of human lamin A interfere with *in vitro* assembly is consistent with the current model, according to which the head-to-tail association of lamin dimers represents the fundamental step in longitudinal self-assembly (Aebi et al., 1986; Herrmann and Aebi, 2004). Presumably, these DARPins inhibit the formation of head-to-tail polymers and therefore keep lamins in a low oligomeric state.

Binding of DARPins to the central coiled-coil domain of lamin A interferes with *in vivo* lamin A/C polymerization and lamina incorporation

The assembly of lamin A/C and its incorporation into the nuclear lamina is not yet understood. Several studies employ lamin A variants that are mutated at distinct amino acids, and thereby have identified sites that are crucial for lamina incorporation. Mutations

Journal of Cell Science

Journal of Cell Science (2015) 128, 3607-3620 doi:10.1242/jcs.171843

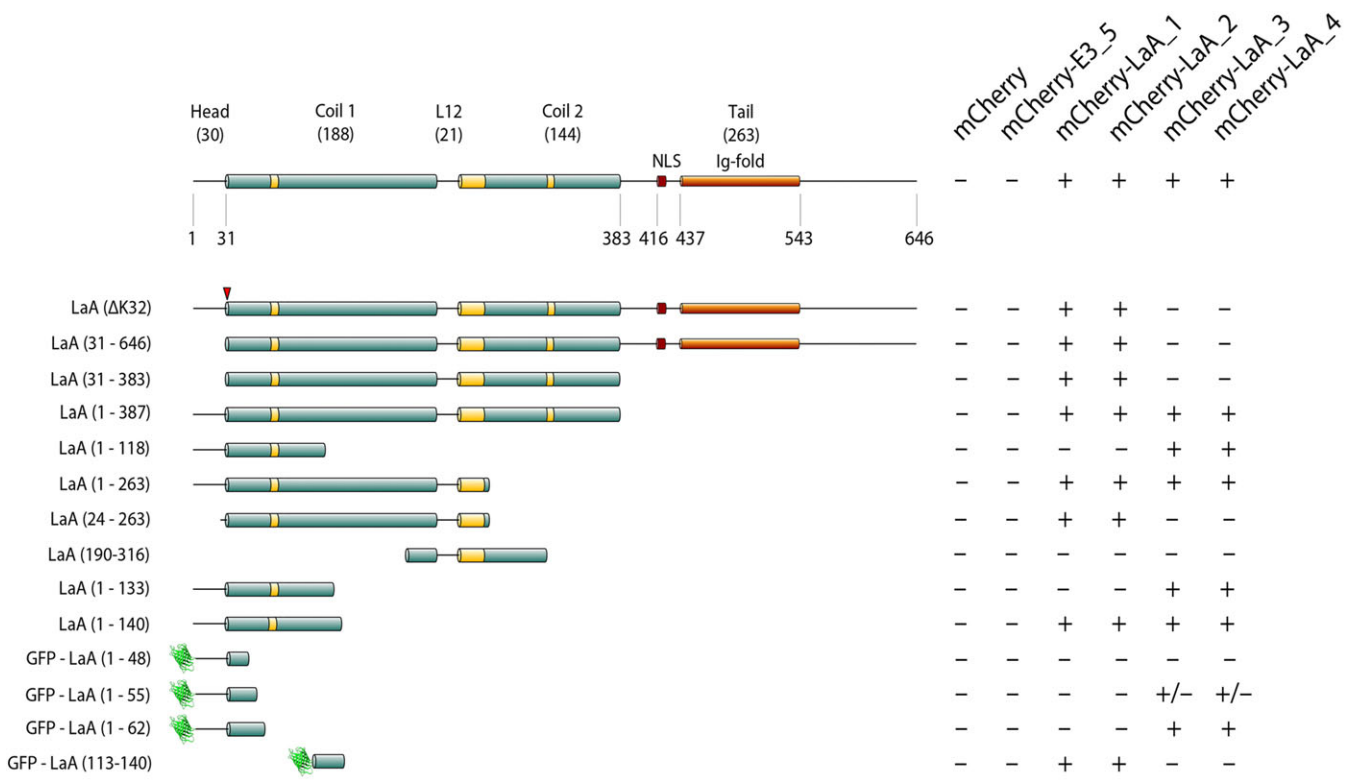

Fig. 6. DARPins selected against lamin A bind to one of two major epitopes. Identification of the binding epitope of four selected DARPins to human lamin A. Top, the protein structure of the full-length mature lamin A. The numbers in brackets represent the number of amino acid residues that comprise the indicated domain. Bottom, selected fragments of lamin A used for epitope mapping (supplementary material Fig. S4). The red arrowhead indicates the position of the deleted amino acid Lys32. Right, +, +/– and – indicate strong, moderate and no detectable DARPin binding to lamin fragments, respectively. DARPins LaA_1 and LaA_2 interacted with amino acids 113–140, and DARPins LaA_3 and LaA_4 bound to amino acids 1–62 of human lamin A. The numbers in brackets represent the number of amino acid residue that comprise the indicated domain.

in the rod domain that alter amino acids L85, N195, E358, M371 and R386 cause impaired lamina assembly, indicating the involvement of the entire rod domain in this process (Holt et al., 2003; Raharjo et al., 2001; Zwerger et al., 2013). Recent studies have found that phosphorylation of amino acid residue Ser22, and to a lesser extent of other phosphosites along the protein, causes a shift in the localization of lamin A from the nuclear envelope to the nucleoplasm and increases mobility (Buxboim et al., 2014; Kochin et al., 2014). However, the distinct steps of lamina incorporation are still elusive, and it remains unclear whether lamin proteins attach to the nuclear lamina as dimers or pre-assembled filaments. Moreover, it is still open as to which components of the nuclear envelope are required to interact with lamin A in order to achieve proper incorporation of lamins into the nuclear lamina.

In this work we show that DARPins that bind to the N-terminal domain of lamin A/C (LaA_3 and LaA_4) do not affect their incorporation into the nuclear lamina, whereas DARPins that interact with A-type lamins through coil 1B of the central rod domain (LaA_1 and LaA_2) cause a substantial delocalization of A-type lamins to the nucleoplasm. Because binding of DARPins LaA_3 and LaA_4 to the lamin A/C head domain does not abolish its nuclear envelope localization *in vivo*, a fully accessible head domain is apparently not required for lamina incorporation.

These results may suggest that (i) the N-terminal domain is required for *in vitro* head-to-tail assembly, whereas *in vivo* assembly requires other domains of lamin A/C, or (ii) that incorporation of A-type lamins into the lamina does not require large filamentous lamin structures. Indeed, to our knowledge there is currently no sufficient evidence that lamin A or lamin C form ‘classic’ filaments in mammalian somatic cells. Only for B-type lamins have such endogenous bona fide filaments been observed, albeit not in mammalian somatic cells but in *Xenopus laevis* oocytes (Aebi et al., 1986; Goldberg et al., 2008). A-type lamin dimers might also polymerize in the form of patches or sheets that might cover a filamentous B-type lamin system.

DARPins LaA_1 and LaA_2 bind to A-type lamins during mitosis and prevent their oligomerization, as judged by ultracentrifugation analyses, as well as their incorporation into the lamina (Fig. 3B; supplementary material Fig. S3A; Fig. 1, Fig. 2A). The nucleoplasmic localization of A-type lamins in these cells is accompanied by high levels of phosphorylated Ser22. One potential explanation might be that DARPin binding blocks substrate recognition or the binding of phosphatases, thereby keeping A-type lamins in a soluble ‘mitotic’ state, in which they are unable to polymerize. However, the latter is less likely because the DARPin-binding site on lamin A/C lies approximately 100 amino acids away from the phosphorylation site. It is also possible that DARPins prevent lamina incorporation by blocking distinct interactions with nuclear envelope components, and thus high levels of phosphorylated Ser22 is not a cause for but a consequence of nucleoplasmic localization.

To address this question, we had expressed the extended DARPin-binding epitope of lamin A/C, amino acid residues 99–147, in HeLa-K cells in order to immunoprecipitate interaction partners of this exact A-type-lamin domain. Despite repeated attempts, however, we did not isolate any cellular binding protein that might interact with the same lamin A/C domain as DARPins LaA_1 and LaA_2 (data not shown). Although we cannot

Journal of Cell Science (2015) 128, 3607-3620 doi:10.1242/jcs.171843

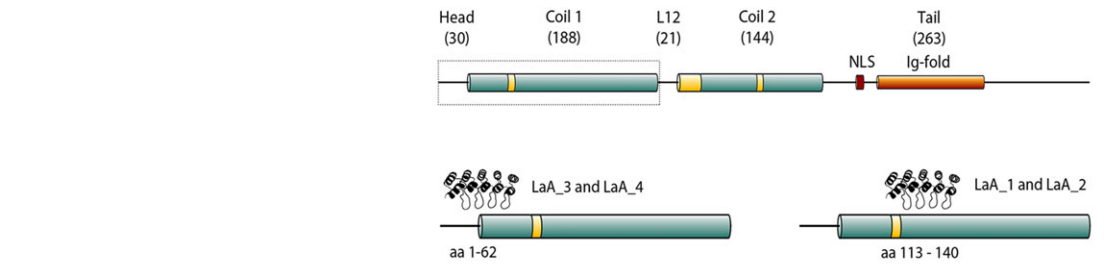

lamin A *in vitro* assembly alterations	+	–
delocalization of lamin A/C from the lamina	–	+
mislocalization of emerin	–	+
mislocalization of lamin B1, Lap2β and NPCs		
in U-2 OS cells	–	–
in HDFs	–	+
aberrant nuclear shape	–	+
decreased nuclear stiffness	–	+

Fig. 7. Two sets of DARPins have different effects on lamin A *in vitro* and on A-type lamins at the cellular level. Summary of the impact of DARPins LaA_1, LaA_2, LaA_3 and LaA_4 on A-type lamins. Top, protein structure of the full-length mature lamin A. The numbers in brackets represent the number of amino acid residues that comprise the indicated domain. The framed lamin A head and coil-1 domain is again depicted enlarged, showing the DARPins binding to the two main epitopes. Bottom, the effects of the two groups of DARPins are summarized. +, indicates effect was observed; –, indicates no effect was observed; aa, amino acid residues; NLS, nuclear localization signal.

exclude the possibility that DARPin binding blocks certain interactions at the nuclear envelope, a thorough investigation of post-translational modifications and phosphatase binding to DARPin LaA_1–lamin A/C complexes might eventually lead to further insights into the *in vivo* assembly of A-type lamins.

Our combined results from *in vitro* and *in vivo* data indicate that incorporation of lamins into the lamina in living cells differs from the assembly of recombinant lamin A. *In vitro* assembly might reflect the homotypic interactions of lamins in the absence of binding partners (Herrmann and Aebi, 2004). In cells, however, lamin-bound chaperones could shield specific domains and thus prevent such interactions. In addition, soluble and membrane-bound lamin-binding partners and additional scaffolding networks might be crucial for ordered *in vivo* lamin assembly.

A-type lamin delocalization to the nuclear interior causes cell-type-dependent nuclear envelope defects and provides a model for testing lamina-dependent and -independent functions of lamin A/C

Expression of DARPins LaA_1 and LaA_2 in cells resulted in the delocalization of lamin A/C from the nuclear lamina to the nucleoplasm. DARPins that interfere with lamin incorporation into the nuclear lamina provide a novel and important tool for differentiating between lamina-dependent and lamina-independent functions of A-type lamins in living human cells. We confirmed the effects of specific DARPins on lamin A/C incorporation into the nuclear lamina in three independent cell lines. Notably, for all cell types, cells that expressed the DARPins LaA_1 and LaA_2 were viable and proliferated. The two cancer cell lines HeLa-K and U2OS cells did not show nuclear envelope alterations, except for a mislocalization of emerin from the nuclear envelope to the cytoplasm, presumably to the ER (Fig. 2A; data not shown). This effect has been previously described in MEFs carrying specific mutations in the *LMNA* gene, as well as in *LMNA*-knockout MEFs. It has been proposed that emerin mislocalization in these cells reflects the requirement of A-type lamins for emerin to be anchored to the nuclear envelope (Nagano et al., 1996; Sullivan et al., 1999). The data provided here further suggests that the anchorage of emerin is a lamina-dependent function and that the pure presence of A-type lamins is insufficient for emerin anchorage.

Notably, lamin A/C delocalization alters several nuclear envelope components in HDFs that are unaffected in cancer cells (Fig. 4A). The phenotype of HDFs that expressed DARPins LaA_1 and LaA_2 is very similar to that described for HDF Y259X cells, which completely lack A-type lamins. Thus, the consequences of loss of A-type lamins are mimicked by inhibiting the incorporation of A-type lamins into the nuclear lamina. In our hands, knockdown of *LMNA* in HDFs repeatedly resulted in cellular growth arrest (data not shown), in agreement with previous reports that have demonstrated that nucleoplasmic LAP2α–lamin-A complexes are required for human fibroblasts to maintain a proliferative state (Pekovic et al., 2007). Our results strengthen this observation, as HDFs that expressed the DARPins LaA_1 and LaA_2, and thus had nucleoplasmic lamin A/C, did not display a proliferation block. Lamin A/C might therefore fulfil a lamina-independent function that is required for proliferation in HDFs but not in cancer cells, further demonstrating cell-type-specific differences in the functions of A-type lamins.

The reasons for cell-type-dependent effects of DARPins that bind to lamin A/C is not entirely clear. We speculate that the composition of nuclear envelope proteins, as well as the presence or absence of nucleoplasmic lamin-binding partners might influence the stability of the nuclear envelope (Korfali et al., 2012). These factors might as well determine the precise functions of lamin A/C in a given cell type. In addition, cancer cells frequently acquire mechanisms to

Journal of Cell Science (2015) 128, 3607-3620 doi:10.1242/jcs.171843

override or reduce the activity of cell cycle checkpoints, which might account for the observation that a proliferation block upon lamin A/C loss occurs only in HDFs, whereas HeLa-K and U2OS cells proliferate normally in the absence of A-type lamins (Helt and Galloway, 2003; Lu et al., 2005; Pekovic et al., 2007). Our study thus emphasizes that observations made in one cell line must be interpreted with caution and cannot be generalized for all cell types.

One major function of lamins is to regulate the mechanical properties of nuclei (Lammerding et al., 2006; Swift et al., 2013). The findings presented here suggest that nuclear shape is dependent on the incorporation of A-type lamins into the lamina, as the nuclear contour ratios of cells that expressed LaA_1 and LaA_2 were comparable to those of cells that lacked A-type lamins (Fig. 5A). Nuclear deformability was increased in cells with nucleoplasmic A-type lamins compared to control cells, but not to the same extent as in cells that lacked A-type lamins. Nucleoplasmic lamin A/C might therefore contribute to nuclear stiffness as well, although these lamins are not assembled into large polymers. Nucleoplasmic A-type lamins form multiple interactions with chromatin and nucleoplasmic factors, such as Lap2α, pRB or PCNA, and might thereby support nuclear stiffness and viscosity (Olins et al., 2009; Simon and Wilson, 2013). Although we cannot exclude the possibility that a minor fraction of lamin A/C is still attached to the nuclear lamina in these cells, it is likely that such amounts would not influence these measurements significantly. Taken together, the mechanical properties of the nucleus mostly rely on the incorporation of A-type lamins into the lamina, although nucleoplasmic lamins presumably play a role in nuclear resistance and strength as well.

In summary, we present here a new approach to alter lamin A/C assembly and localization, based on DARPin technology. Different DARPins inhibit the assembly of A-type lamins into higher order structures either *in vitro* or *in vivo* and, thus, contribute to a more differentiated description of lamin functions. Moreover, the use of specific lamin-binding proteins enables the study of the effect of distinct domains on protein interactions at the nuclear envelope, without altering the lamin expression level. This innovative approach can further be adopted for biochemical, biophysical and cell biology studies of other IF proteins, and might shed light on their cellular assemblies and functions.

MATERIALS AND METHODS

Plasmids

For DARPin selection, human mature lamin A (LMNA, UniProt accession number P02545), was cloned with an N-terminal 6×His–TEV site and a C-terminal AVI-tag in pET24d(+) (Novagen) to generate $_{6His\text{-}TEV}laminA_{Avi}$.

For protein expression, the coding sequences of DARPins were cloned into pQE-30 (Qiagen) modified with an additional Myc-tag ($_{6His}DARPins_{Myc}$), or into the standard vector pQE-30 ($_{6His}$DARPins). For eukaryotic expression, coding sequences of selected DARPins were cloned into pIRES-GFP or mCherry-C1 ($_{mCherry}$DARPins, both Clontech). Selected $_{mCherry}$DARPins were amplified from the mCherry-C1 plasmid and ligated into the pET24d(+) with N-terminal 6×His–TEV site ($_{6His\text{-}TEV\text{-}mCherry}$DARPins).

For lentiviral transduction, a pCDH-CMV-MCS-EF1-puro (SBI) was modified to pCDH-CMV-MCS-IRES-copGFP-EF1-puro, and human lamin A, lamin C and 6×His-tagged DARPins ($_{6His}$DARPins) were cloned into this vector.

For epitope characterization, human lamin A, lamin A ΔK32 and lamin A domain-truncated variants were ligated into pET24a(+) plasmid (Novagen) without a tag, with N-terminal 6×His-TEV ($_{6His\text{-}TEV}$LaA fragments), or, for short lamin A fragments, with N-terminal 6×His–TEV site ($_{6His\text{-}TEV\text{-}GFP}$LaA fragments). Full-length clones of lamin B1 and lamin B2 (Schumacher et al., 2006), keratins, desmin or vimentin were subcloned into pET24a(+). All vector modifications were verified by Sanger sequencing.

Ribosome display, crude extract ELISA and surface plasmon resonance analysis

For selection of lamin-A-specific DARPins, an N_3C library was used, and four standard ribosome-display selection rounds (Seeger et al., 2013) were performed against immobilized $_{6His\text{-}TEV}laminA_{Avi}$, reconstituted in a 'dimerization buffer' containing 300 mM NaCl, 25 mM Tris (pH 8.0), 2 mM EDTA and 1 mM DTT (Herrmann and Aebi, 2004; Taimen et al., 2009). Crude extract ELISA against reconstituted $_{6His\text{-}TEV}laminA_{Avi}$ and surface plasmon resonance analysis on a Proteon XPR36TM (Bio-Rad Laboratories, Inc.) was performed as described previously (Seeger et al., 2013).

Cell culture and cell treatment

HeLa-K cells, human osteosarcoma cells (U2OS; American Type Culture Collection number HTB-96), HEK-293T cells, wild-type HDFs (Muchir et al., 2004) and human fibroblasts carrying a homozygous nonsense Y259X mutation in lamin A/C (van Engelen et al., 2005) were maintained in Dulbecco's modified Eagle's medium supplemented with 10% fetal bovine serum, 2 mM L-glutamine, 100 U/ml penicillin and 100 µg/ml streptomycin.

For induction of lamin A/C hyperphosphorylation, cells were arrested in G2/M phase by treatment with 100 ng/ml nocodazole for 20 h, and mitotic cells were collected by mitotic shake-off. To inhibit protein synthesis, translation was blocked by treating cells with 100 µg/ml cycloheximide for 6, 12 or 24 h.

Cell line modifications

All modified HeLa-K cells presented – except for HeLa-K cells with stable knockdown – were modified through transfection with Fugene HD transfection reagent (Promega). At 24 h after transfection, positive cells were selected by addition of Geneticin (Life Technologies) at a concentration of 1.5 mg/ml to the culture medium for 2–3 weeks. To increase the fraction of positive cells, cells were sorted for the bicistronically expressed GFP or for the mCherry-tag by using fluorescence activated cell sorting (FACS) at the ZMB Center for Microscopy and Image Analysis (University of Zurich). U2OS cells, HDFs and HeLa-K cells were modified through lentiviral infection [in the case of HeLa-K, cells were modified for stable knockdown of lamin A/C (Sigma mission, clone number NM_170707.1-752s1c1) and for the respective scrambled control] using HEK-293T cells as packaging cells and the packaging vectors dMD2.G and psPAX2 (Addgene), and following the Purefection protocol for Lentiviral packaging (System Biosciences). 4 µg/ml puromycin (Invitrogen) was added to the medium for selection of positive cells, and cell lines were subsequently maintained in this selection medium.

Immunofluorescence and western blot analysis

Immunofluorescence and western blot analysis, including sample preparation, were performed as previously described (Zwerger et al., 2010). The following antibodies were used in this study: mouse anti-lamin A/C (LaZ, Geiger et al., 2008), mouse anti-lamin A/C (clone 636, Santa Cruz), goat anti-lamin B1 (clone M-20, Santa Cruz), mouse anti-lamin B2 (clone X223; Progen), guinea pig serum against LBR (LBR N-term, Cohen et al., 2008), guinea pig serum against emerin (Em-N-term, Dreger et al., 2002), guinea pig serum against Lap2α, mouse anti-Lap2β (mAb 16, Dechat et al., 1998), rabbit anti-phosphorylated-Ser22 lamin A/C, mouse anti-β-actin (catalog number A5441, Sigma-Aldrich), and mouse antibody against red fluorescent protein (RFP; 3F5, Chromotek). FITC-, Cy3-, Cy5-, Alexa488-, Alexa647- or peroxidase-conjugated secondary antibodies were purchased from Jackson ImmunoResearch Laboratory. Primary and secondary antibody dilutions were as recommended by the supplier.

Protein expression and purification

Biotinylated $_{6His\text{-}TEV}laminA_{Avi}$ was generated through co-expression with a plasmid containing the coding sequence for BirA in BL21-CodonPlus (DE3) grown in terrific broth (Difco™ Terrific Broth) after induction with 1 mM isopropyl β-D-1-thiogalactopyranoside (IPTG) for approximately 3 h at 37°C in the presence of biotin (Sigma-Aldrich); protein was then

purified under denaturing conditions following the protocol of the QiaExpressionist (Qiagen).

$_{6His}$DARPins (~18 kDa) and $_{6His\text{-}TEV\text{-}mCherry}$DARPins (~45 kDa) were expressed in BL21-CodonPlus(DE3) grown in terrific broth after induction with 1 mM IPTG for approximately 5 h at 37°C and 16 h at 18°C, respectively, and purified as previously described (Seeger et al., 2013).

The plasmids encoding the human lamin A fragments comprising amino acids 1–118, 1–263, 24–263, 190–316 and 264–402 in a pPEP-TEV vector [$_{ppep\text{-}6His\text{-}TEV}$LaA fragments, kind gift of Larisa Kapinos, Biozentrum, University of Basel, Switzerland (Kapinos et al., 2010)], as well as those encoding the $_{6His\text{-}TEV}$LaA fragments and $_{6His\text{-}TEV\text{-}GFP}$LaA fragments were transformed into *E. coli* BL21-CodonPlus(DE3). Bacteria were cultured in terrific broth, and protein expression was induced with 1 mM IPTG for 4–6 h at 37°C. The untagged recombinant human proteins mature lamin A, lamin A 1–646 Δ32, domain-deleted lamin A variants, lamin C, lamin B1 and lamin B2 were expressed and purified from BL21-CodonPlus(DE3) as described (Taimen et al., 2009). Keratins, vimentin, desmin and neurofilament L in a pET24a(+) vector were expressed and purified as previously described (Herrmann et al., 2004, 2002).

Epitope characterization

For epitope characterization, protein samples of human lamin A or lamin A fragments were loaded onto NuPAGE® Novex® 4–12% Bis-Tris gels (LifeTechnologies) and either Coomassie-stained or blotted onto Immobilon PVFD membranes (Millipore). Membranes were blocked in PBST (PBS with 0.05% Tween-20) with 5% non-fat dried milk and incubated with purified $_{6His\text{-}TEV\text{-}}$mCherry or $_{6His\text{-}TEV\text{-}mCherry}$DARPins at a concentration of 100 µg/ml for 2 h. Bound proteins were detected with an anti-RFP antibody. For testing DARPin binding to IF proteins, purified, untagged human lamin A, lamin C, lamin B1 and lamin B2, keratin 5, keratin 8, keratin 14, keratin 18, vimentin, desmin and neurofilament L were loaded onto 4–12% Bis-Tris Gels. Analysis of DARPin binding was performed as described above.

In vitro assembly

In vitro assembly of human lamin A was performed as previously described with a few modifications (Zwerger et al., 2013). In brief, human lamin A in dimerization buffer at a concentration of 0.2 mg/ml was incubated with an excess of $_{6His}$DARPins that were dialyzed into the same buffer (at least 4× molar concentration) at room temperature for 1 h. Paracrystal assembly was initiated by a stepwise reduction of the salt concentration from 300 to 50 mM NaCl. Samples were centrifuged for 35 min at 50,000 ***g*** and 4°C. Proteins in the supernatants were precipitated using Trichloroacetic acid (TCA), and pelleted supernatant, as well as pellets, were resuspended in Laemmli sample buffer and boiled for 5 min at 95°C. The entire samples were separated on 12.5% SDS gels and Coomassie-stained. For specific $_{6His}$DARPins, the assay was performed in three individual experiments.

Co-immunoprecipitation assay and mass spectrometry analysis

Cells were lysed for 20 min on ice with RIPA buffer [150 mM NaCl, 50 mM Tris-HCl (pH 8.0), 1% NP-40, 0.1% sodium dodecyl sulfate, 0.5% sodium deoxycholate, 0.5 mM EDTA] supplemented with cOmplete protease inhibitor (Roche), 10 mg/ml Pefabloc and 4 mg/ml DNAse I. Lysates were cleared by centrifuging, and supernatants were diluted in a 1:5 ratio with 'Immunoprecipitation wash buffer' containing 150 mM NaCl, 50 mM Tris-HCl (pH 8.0), 0.5 mM EDTA and protease inhibitor, to a final concentration of 0.2% NP-40, 0.02% sodium dodecyl sulfate and 0.1% sodium deoxycholate. Diluted lysates were incubated with equilibrated RFP-Trap_A beads (Chromotek) for 2 h at 4°C, then washed with 1:5 diluted RIPA buffer, followed by several washing steps with immunoprecipitation wash buffer. Bound proteins were eluted through addition of pre-heated Laemmli sample buffer to the beads and incubation for 5 min at 95°C. For western blot analysis, lysates of approximately 6.2×10^5 cells and precipitates of approximately 2×10^4 cells were loaded onto 10% SDS gels, representing an approximate 30:1 ratio of lysates (input) to immunoprecipitates. For mass spectrometry analysis, precipitates of approximately 2×10^7 cells were loaded onto a 4–12% Bis-Tris gel. The gel was Coomassie-stained and the three major protein bands that co-immunoprecipitated with $_{mCherry}$DARPins were excised. Mass spectrometry analysis was performed at the Functional Genomics Center Zurich.

Differential protein extraction

Approximately 3×10^6 cells were resuspended in 200 µl of lysis buffer containing 0.5× PBS, 50 mM MOPS (pH 7.0), 10 mM $MgCl_2$, 1 mM EGTA, 0.2% NP40, cOmplete protease inhibitor and 0.75% saturated PMSF in ethanol. Extraction with 0.2–1% NP40 detergent has been previously shown to release only a small lamin A/C fraction but not lamina-associated A-type lamins (Kolb et al., 2011). Extraction was performed at 4°C for 5 min. Insoluble cellular components were briefly spun down, and the supernatant was boiled with Laemmli sample buffer. Alternatively, a part of the supernatant was additionally centrifuged at 50,000 ***g*** for 35 min at 4°C, then the supernatant was boiled with Laemmli sample buffer. The insoluble fraction was boiled for 5 min at 95°C with urea sample buffer (10 M urea in 1.5× Laemmli sample buffer), and a 1:10 dilution of the pellet sample was prepared. Supernatant and 1:10-diluted pellet fractions were separated on a 4–12% Bis-Tris gels. Differential extractions were performed independently three times and quantified using ImageJ.

Nuclear shape analysis and nuclear strain analysis

For a quantitative assessment of the nuclear shape, the nuclear cross-sectional area and perimeter of Hoechst-33342-stained nuclei was measured using a custom-written MATLAB program (Lombardi et al., 2011). The program automatically calculates the nuclear contour ratio ($4\pi\times$area/perimeter^2), yielding a quantitative measure of nuclear roundness (Lammerding et al., 2005). More than 300 nuclei from cells with substantial green fluorescence (the bicistronically expressed GFP is a marker for expression levels of DARPins) were analyzed per cell line.

To analyze the nuclear stiffness, we measured nuclear deformations in response to substrate strain application and calculated the normalized nuclear strain as described previously (Lombardi et al., 2011). Per cell line, ≥100 nuclei from cells with substantial green fluorescence were analyzed.

Acknowledgements

We thank Larisa Kapinos, Monika Mauermann, Philipp Isermann, Roland Foisner, Thomas Dechat, Robert Goldman, Stephen Adam and Gisele Bonne for generously providing us with protein and DNA material, as well as with antibodies; we thank Howard Worman, Jos Broers, Baziel van Engelen, Urs Greber and Ulrike Kutay for providing us with fibroblasts, HeLa-K and U2OS cell lines. We are grateful to Urs Greber for help in conducting viral transduction experiments, and the ZMB Center for Microscopy and Image Analysis for their support.

Competing interests

The authors declare no competing or financial interests.

Author contributions

M.Z., H.R.-V. and O.M. designed the experiments and interpreted the data being published. M.Z., H.R.-V. and R.Z. executed the experiments. C.D. generated a cell line for the study. J.L, H.H. and M.G.G. contributed to the design of the experiments and interpretation of the data. M.Z., O.M., J.L. and H.H. contributed to the writing of the article.

Funding

The work was supported by a Swiss National Science Foundation grant [grant number SNSF 31003A_141083/1 (to O.M.)]; a postdoctoral fellowship from the German Academic Exchange Service (DAAD) [grant number D/11/44980 to M.Z.]; the European Commission's Seventh Framework Programme [grant number FP7/2007–2013]; P-CUBE under grant agreement number 227764 (Programme P-CUBE); funding from the National Institutes of Health [grant numbers R01 NS059348 and R01 HL082792]; the National Science Foundation [CAREER award grant number CBET-1254846]; and the Department of Defense (Breast Cancer Idea Award) [grant number BC102152 (to J.L.)]. Deposited in PMC for release after 12 months.

Supplementary material

Supplementary material available online at
http://jcs.biologists.org/lookup/suppl/doi:10.1242/jcs.171843/-/DC1

References

Aebi, U., Cohn, J., Buhle, L. and Gerace, L. (1986). The nuclear lamina is a meshwork of intermediate-type filaments. *Nature* **323**, 560-564.

Ben-Harush, K., Wiesel, N., Frenkiel-Krispin, D., Moeller, D., Soreq, E., Aebi, U., Herrmann, H., Gruenbaum, Y. and Medalia, O. (2009). The supramolecular organization of the C. elegans nuclear lamin filament. *J. Mol. Biol.* **386**, 1392-1402.

Bertrand, A. T., Chikhaoui, K., Yaou, R. B. and Bonne, G. (2011). Clinical and genetic heterogeneity in laminopathies. *Biochem. Soc. Trans.* **39**, 1687-1692.

Binz, H. K., Amstutz, P., Kohl, A., Stumpp, M. T., Briand, C., Forrer, P., Grütter, M. G. and Plückthun, A. (2004). High-affinity binders selected from designed ankyrin repeat protein libraries. *Nat. Biotechnol.* **22**, 575-582.

Binz, H. K., Kohl, A., Plückthun, A. and Grütter, M. G. (2006). Crystal structure of a consensus-designed ankyrin repeat protein: implications for stability. *Proteins* **65**, 280-284.

Burke, B. and Stewart, C. L. (2013). The nuclear lamins: flexibility in function. *Nat. Rev. Mol. Cell Biol.* **14**, 13-24.

Buxboim, A., Swift, J., Irianto, J., Spinler, K. R., Dingal, P. C. D. P., Athirasala, A., Kao, Y.-R., Cho, S., Harada, T., Shin, J.-W. et al. (2014). Matrix elasticity regulates lamin-A,C phosphorylation and turnover with feedback to actomyosin. *Curr. Biol.* **24**, 1909-1917.

Cohen, T. V., Klarmann, K. D., Sakchaisri, K., Cooper, J. P., Kuhns, D., Anver, M., Johnson, P. F., Williams, S. C., Keller, J. R. and Stewart, C. L. (2008). The lamin B receptor under transcriptional control of C/EBPepsilon is required for morphological but not functional maturation of neutrophils. *Hum. Mol. Genet.* **17**, 2921-2933.

Dechat, T., Gotzmann, J., Stockinger, A., Harris, C. A., Talle, M. A., Siekierka, J. J. and Foisner, R. (1998). Detergent-salt resistance of LAP2alpha in interphase nuclei and phosphorylation-dependent association with chromosomes early in nuclear assembly implies functions in nuclear structure dynamics. *EMBO J.* **17**, 4887-4902.

Dechat, T., Pfleghaar, K., Sengupta, K., Shimi, T., Shumaker, D. K., Solimando, L. and Goldman, R. D. (2008). Nuclear lamins: major factors in the structural organization and function of the nucleus and chromatin. *Genes Dev.* **22**, 832-853.

Dechat, T., Adam, S. A., Taimen, P., Shimi, T. and Goldman, R. D. (2010a). Nuclear lamins. *Cold Spring Harb. Perspect. Biol.* **2**, a000547.

Dechat, T., Gesson, K. and Foisner, R. (2010b). Lamina-independent lamins in the nuclear interior serve important functions. *Cold Spring Harb. Symp. Quant. Biol.* **75**, 533-543.

Dhe-Paganon, S., Werner, E. D., Chi, Y.-I. and Shoelson, S. E. (2002). Structure of the globular tail of nuclear lamin. *J. Biol. Chem.* **277**, 17381-17384.

Dorner, D., Vlcek, S., Foeger, N., Gajewski, A., Makolm, C., Gotzmann, J., Hutchison, C. J. and Foisner, R. (2006). Lamina-associated polypeptide 2alpha regulates cell cycle progression and differentiation via the retinoblastoma-E2F pathway. *J. Cell Biol.* **173**, 83-93.

Dorner, D., Gotzmann, J. and Foisner, R. (2007). Nucleoplasmic lamins and their interaction partners, LAP2alpha, Rb, and BAF, in transcriptional regulation. *FEBS J.* **274**, 1362-1373.

Dreger, C. K., König, A. R., Spring, H., Lichter, P. and Herrmann, H. (2002). Investigation of nuclear architecture with a domain-presenting expression system. *J. Struct. Biol.* **140**, 100-115.

Geiger, S. K., Bär, H., Ehlermann, P., Wälde, S., Rutschow, D., Zeller, R., Ivandic, B. T., Zentgraf, H., Katus, H. A., Herrmann, H. et al. (2008). Incomplete nonsense-mediated decay of mutant lamin A/C mRNA provokes dilated cardiomyopathy and ventricular tachycardia. *J. Mol. Med.* **86**, 281-289.

Goldberg, M. W., Huttenlauch, I., Hutchison, C. J. and Stick, R. (2008). Filaments made from A- and B-type lamins differ in structure and organization. *J. Cell Sci.* **121**, 215-225.

Heald, R. and McKeon, F. (1990). Mutations of phosphorylation sites in lamin A that prevent nuclear lamina disassembly in mitosis. *Cell* **61**, 579-589.

Helt, A.-M. and Galloway, D. A. (2003). Mechanisms by which DNA tumor virus oncoproteins target the Rb family of pocket proteins. *Carcinogenesis* **24**, 159-169.

Herrmann, H. and Aebi, U. (2004). Intermediate filaments: molecular structure, assembly mechanism, and integration into functionally distinct intracellular Scaffolds. *Annu. Rev. Biochem.* **73**, 749-789.

Herrmann, H., Wedig, T., Porter, R. M., Lane, E. B. and Aebi, U. (2002). Characterization of early assembly intermediates of recombinant human keratins. *J. Struct. Biol.* **137**, 82-96.

Herrmann, H., Kreplak, L. and Aebi, U. (2004). Isolation, characterization, and in vitro assembly of intermediate filaments. *Methods Cell Biol.* **78**, 3-24.

Herrmann, H., Bär, H., Kreplak, L., Strelkov, S. V. and Aebi, U. (2007). Intermediate filaments: from cell architecture to nanomechanics. *Nat. Rev. Mol. Cell Biol.* **8**, 562-573.

Holt, I., Ostlund, C., Stewart, C. L., thi Man, N., Worman, H. J. and Morris, G. E. (2003). Effect of pathogenic mis-sense mutations in lamin A on its interaction with emerin in vivo. *J. Cell Sci.* **116**, 3027-3035.

Isobe, K., Gohara, R., Ueda, T., Takasaki, Y. and Ando, S. (2007). The last twenty residues in the head domain of mouse lamin A contain important structural elements for formation of head-to-tail polymers in vitro. *Biosci. Biotechnol. Biochem.* **71**, 1252-1259.

Kapinos, L. E., Schumacher, J., Mücke, N., Machaidze, G., Burkhard, P., Aebi, U., Strelkov, S. V. and Herrmann, H. (2010). Characterization of the head-to-tail overlap complexes formed by human lamin A, B1 and B2 "half-minilamin" dimers. *J. Mol. Biol.* **396**, 719-731.

Kochin, V., Shimi, T., Torvaldson, E., Adam, S. A., Goldman, A., Pack, C.-G., Melo-Cardenas, J., Imanishi, S. Y., Goldman, R. D. and Eriksson, J. E. (2014). Interphase phosphorylation of lamin A. *J. Cell Sci.* **127**, 2683-2696.

Kolb, T., Maass, K., Hergt, M., Aebi, U. and Herrmann, H. (2011). Lamin A and lamin C form homodimers and coexist in higher complex forms both in the nucleoplasmic fraction and in the lamina of cultured human cells. *Nucleus* **2**, 425-433.

Korfali, N., Wilkie, G. S., Swanson, S. K., Srsen, V., de Las Heras, J., Batrakou, D. G., Malik, P., Zuleger, N., Kerr, A. R. W., Florens, L. et al. (2012). The nuclear envelope proteome differs notably between tissues. *Nucleus* **3**, 552-564.

Lammerding, J., Schulze, P. C., Takahashi, T., Kozlov, S., Sullivan, T., Kamm, R. D., Stewart, C. L. and Lee, R. T. (2004). Lamin A/C deficiency causes defective nuclear mechanics and mechanotransduction. *J. Clin. Invest.* **113**, 370-378.

Lammerding, J., Hsiao, J., Schulze, P. C., Kozlov, S., Stewart, C. L. and Lee, R. T. (2005). Abnormal nuclear shape and impaired mechanotransduction in emerin-deficient cells. *J. Cell Biol.* **170**, 781-791.

Lammerding, J., Fong, L. G., Ji, J. Y., Reue, K., Stewart, C. L., Young, S. G. and Lee, R. T. (2006). Lamins A and C but not lamin B1 regulate nuclear mechanics. *J. Biol. Chem.* **281**, 25768-25780.

Lin, F. and Worman, H. J. (1993). Structural organization of the human gene encoding nuclear lamin A and nuclear lamin C. *J. Biol. Chem.* **268**, 16321-16326.

Loewinger, L. and McKeon, F. (1988). Mutations in the nuclear lamin proteins resulting in their aberrant assembly in the cytoplasm. *EMBO J.* **7**, 2301-2309.

Lombardi, M. L., Zwerger, M. and Lammerding, J. (2011). Biophysical assays to probe the mechanical properties of the interphase cell nucleus: substrate strain application and microneedle manipulation. *J. Vis. Exp.*

Lu, X., Nannenga, B. and Donehower, L. A. (2005). PPM1D dephosphorylates Chk1 and p53 and abrogates cell cycle checkpoints. *Genes Dev.* **19**, 1162-1174.

Muchir, A., Medioni, J., Laluc, M., Massart, C., Arimura, T., van der Kooi, A. J., Desguerre, I., Mayer, M., Ferrer, X., Briault, S. et al. (2004). Nuclear envelope alterations in fibroblasts from patients with muscular dystrophy, cardiomyopathy, and partial lipodystrophy carrying lamin A/C gene mutations. *Muscle Nerve* **30**, 444-450.

Nagano, A., Koga, R., Ogawa, M., Kurano, Y., Kawada, J., Okada, R., Hayashi, Y. K., Tsukahara, T. and Arahata, K. (1996). Emerin deficiency at the nuclear membrane in patients with Emery-Dreifuss muscular dystrophy. *Nat. Genet.* **12**, 254-259.

Olins, A. L., Hoang, T. V., Zwerger, M., Herrmann, H., Zentgraf, H., Noegel, A. A., Karakesisoglou, I., Hodzic, D. and Olins, D. E. (2009). The LINC-less granulocyte nucleus. *Eur. J. Cell Biol.* **88**, 203-214.

Otterbein, L. R., Graceffa, P. and Dominguez, R. (2001). The crystal structure of uncomplexed actin in the ADP state. *Science* **293**, 708-711.

Parry, D. A. D. (2005). Microdissection of the sequence and structure of intermediate filament chains. *Adv. Protein Chem.* **70**, 113-142.

Pekovic, V., Harborth, J., Broers, J. L. V., Ramaekers, F. C. S., van Engelen, B., Lammens, M., von Zglinicki, T., Foisner, R., Hutchison, C. and Markiewicz, E. (2007). Nucleoplasmic LAP2alpha-lamin A complexes are required to maintain a proliferative state in human fibroblasts. *J. Cell Biol.* **176**, 163-172.

Pereira, S., Bourgeois, P., Navarro, C., Esteves-Vieira, V., Cau, P., De Sandre-Giovannoli, A. and Lévy, N. (2008). HGPS and related premature aging disorders: from genomic identification to the first therapeutic approaches. *Mech. Ageing Dev.* **129**, 449-459.

Peter, M., Kitten, G. T., Lehner, C. F., Vorburger, K., Bailer, S. M., Maridor, G. and Nigg, E. A. (1989). Cloning and sequencing of cDNA clones encoding chicken lamins A and B1 and comparison of the primary structures of vertebrate A- and B-type lamins. *J. Mol. Biol.* **208**, 393-404.

Pollard, T. D. (2007). Regulation of actin filament assembly by Arp2/3 complex and formins. *Annu. Rev. Biophys. Biomol. Struct.* **36**, 451-477.

Raharjo, W. H., Enarson, P., Sullivan, T., Stewart, C. L. and Burke, B. (2001). Nuclear envelope defects associated with LMNA mutations cause dilated cardiomyopathy and Emery-Dreifuss muscular dystrophy. *J. Cell Sci.* **114**, 4447-4457.

Schumacher, J., Reichenzeller, M., Kempf, T., Schnölzer, M. and Herrmann, H. (2006). Identification of a novel, highly variable amino-terminal amino acid sequence element in the nuclear intermediate filament protein lamin B(2) from higher vertebrates. *FEBS Lett.* **580**, 6211-6216.

Seeger, M. A., Zbinden, R., Flütsch, A., Gutte, P. G., Engeler, S., Roschitzki-Voser, H. and Grütter, M. G. (2013). Design, construction, and characterization of a second-generation DARP in library with reduced hydrophobicity. *Protein Sci.* **22**, 1239-1257.

Shimi, T., Pfleghaar, K., Kojima, S.-I., Pack, C.-G., Solovei, I., Goldman, A. E., Adam, S. A., Shumaker, D. K., Kinjo, M., Cremer, T. et al. (2008). The A- and B-

type nuclear lamin networks: microdomains involved in chromatin organization and transcription. *Genes Dev.* **22**, 3409-3421.

Shumaker, D. K., Lopez-Soler, R. I., Adam, S. A., Herrmann, H., Moir, R. D., Spann, T. P. and Goldman, R. D. (2005). Functions and dysfunctions of the nuclear lamin Ig-fold domain in nuclear assembly, growth, and Emery-Dreifuss muscular dystrophy. *Proc. Natl. Acad. Sci. USA* **102**, 15494-15499.

Simon, D. N. and Wilson, K. L. (2013). Partners and post-translational modifications of nuclear lamins. *Chromosoma* **122**, 13-31.

Spann, T. P., Moir, R. D., Goldman, A. E., Stick, R. and Goldman, R. D. (1997). Disruption of nuclear lamin organization alters the distribution of replication factors and inhibits DNA synthesis. *J. Cell Biol.* **136**, 1201-1212.

Stick, R. and Goldberg, M. W. (2010). Oocytes as an experimental system to analyze the ultrastructure of endogenous and ectopically expressed nuclear envelope components by field-emission scanning electron microscopy. *Methods* **51**, 170-176.

Sullivan, T., Escalante-Alcalde, D., Bhatt, H., Anver, M., Bhat, N., Nagashima, K., Stewart, C. L. and Burke, B. (1999). Loss of A-type lamin expression compromises nuclear envelope integrity leading to muscular dystrophy. *J. Cell Biol.* **147**, 913-920.

Svitkina, T. M. and Borisy, G. G. (1999). Arp2/3 complex and actin depolymerizing factor/cofilin in dendritic organization and treadmilling of actin filament array in lamellipodia. *J. Cell Biol.* **145**, 1009-1026.

Swift, J., Ivanovska, I. L., Buxboim, A., Harada, T., Dingal, P. C. D. P., Pinter, J., Pajerowski, J. D., Spinler, K. R., Shin, J.-W., Tewari, M. et al. (2013). Nuclear lamin-A scales with tissue stiffness and enhances matrix-directed differentiation. *Science* **341**, 1240104.

Taimen, P., Pfleghaar, K., Shimi, T., Moller, D., Ben-Harush, K., Erdos, M. R., Adam, S. A., Herrmann, H., Medalia, O., Collins, F. S. et al. (2009). A progeria mutation reveals functions for lamin A in nuclear assembly, architecture, and chromosome organization. *Proc. Natl. Acad. Sci. USA* **106**, 20788-20793.

Thompson, L. J., Bollen, M. and Fields, A. P. (1997). Identification of protein phosphatase 1 as a mitotic lamin phosphatase. *J. Biol. Chem.* **272**, 29693-29697.

van Engelen, B. G. M., Muchir, A., Hutchison, C. J., van der Kooi, A. J., Bonne, G. and Lammens, M. (2005). The lethal phenotype of a homozygous nonsense mutation in the lamin A/C gene. *Neurology* **64**, 374-376.

Vorburger, K., Lehner, C. F., Kitten, G. T., Eppenberger, H. M. and Nigg, E. A. (1989). A second higher vertebrate B-type lamin: cDNA sequence determination and in vitro processing of chicken lamin B2. *J. Mol. Biol.* **208**, 405-415.

Worman, H. J. (2012). Nuclear lamins and laminopathies. *J. Pathol.* **226**, 316-325.

Worman, H. J., Lazaridis, I. and Georgatos, S. D. (1988). Nuclear lamina heterogeneity in mammalian cells. Differential expression of the major lamins and variations in lamin B phosphorylation. *J. Biol. Chem.* **263**, 12135-12141.

Wurzenberger, C. and Gerlich, D. W. (2011). Phosphatases: providing safe passage through mitotic exit. *Nat. Rev. Mol. Cell Biol.* **12**, 469-482.

Zwerger, M. and Medalia, O. (2013). From lamins to lamina: a structural perspective. *Histochem. Cell Biol.* **140**, 3-12.

Zwerger, M., Kolb, T., Richter, K., Karakesisoglou, I. and Herrmann, H. (2010). Induction of a massive endoplasmic reticulum and perinuclear space expansion by expression of lamin B receptor mutants and the related sterol reductases TM7SF2 and DHCR7. *Mol. Biol. Cell* **21**, 354-368.

Zwerger, M., Jaalouk, D. E., Lombardi, M. L., Isermann, P., Mauermann, M., Dialynas, G., Herrmann, H., Wallrath, L. L. and Lammerding, J. (2013). Myopathic lamin mutations impair nuclear stability in cells and tissue and disrupt nucleo-cytoskeletal coupling. *Hum. Mol. Genet.* **22**, 2335-2349.

Journal of Cell Science